# Three-Dimensional Modeling of Lung Volumes in Application to Scoliosis

Authors:
Dana Wang
Alma Rivera
Madison Goldrich
Termeh Ahi
Dr. Keith Bachmann
Dr. Jeffrey Holmes
Dr. Gustavo Rohde

Words:
Number of Figures: 8
Number of Tables: 1
Number of Equations: 0
Number of Supplements: 1
Number of References: 16

Approved: _____ Date: 4/27/20

Keith Bachmann, Department of Orthopaedic Surgery

# Three-Dimensional Modeling of Lung Volumes in Application to Scoliosis

**Dana Wang[a], Alma Rivera[a], Madison Goldrich[a], Termeh Ahi[a], Keith Bachmann[b], Jeffrey Holmes[a], Gustavo Rohde[a,c]**

[a] Biomedical Engineering, University of Virginia
[b] Department of Orthopedic Surgery, University of Virginia
[c] Electrical and Computer Engineering, University of Virginia

## Abstract

Adolescent idiopathic scoliosis is a curvature of the spine, which also distorts the ribcage and can lead to partial loss of lung function. In order to determine which of two surgical interventions to use on their patients - one temporary, one permanent - physicians must know the condition of their patients' lung development. This is determined by measuring lung volume using CT scans which have negative radiation effects on children. Thus, this Capstone paper presents two major steps towards developing a novel computational model that uses X-ray images as a safer method to calculate patient lung volume. The first step consisted of obtaining mediastinal volumes from patient CT scans using the Pulmonary Toolkit in MATLAB. It was found that weight is the highest predictor of mediastinal volume in both male and female patients and that the mediastinal volume prediction is most accurate when both age and weight are taken into account. The second step involved the construction of a 3-dimensional ribcage model using MATLAB. The preliminary ribcage model was built using the Image Processing Toolbox, and X-ray image clustering was performed using the kmeans algorithm. There is a need for further testing to determine which reconstruction method, maximal intensity projection or volume rendering, is optimal for building the standardized ribcage model from CT scans. Further, it was determined that clustering is a promising technique to obtain X-ray coordinates for morphing the standardized ribcage model to individual patients, but there is a need for future investigators to optimize clustering. Future Capstone groups will be able to build upon this work in order to ultimately calculate lung volume by subtracting mediastinal constants from thoracic volumes found using the ribcage model and validate the accuracy of this framework.

Keywords: Adolescent Idiopathic Scoliosis, Mediastinum, 3D Ribcage Model

## Introduction

Scoliosis is a medical condition that affects approximately 2-4% of adolescents and can be classified as either congenital: in which the spine does not fully develop in the womb, neuromuscular: caused by a neurological or muscular disorder, or idiopathic: wherein the spine shape changes as the child grows.[1] Of the approximate seven to nine million cases of adolescent scoliosis in the United States, about 85% are classified as idiopathic scoliosis cases.[2,3] Scoliosis is defined as an abnormal curvature of the spine that typically grows in an elongated "S" or "C" shape and causes simultaneous sideways curving and twisting of the spine.[4] This can result in visual deformity, emotional distress, back pain, and respiratory impairment. Respiratory impairment occurs because of the complex effects of scoliosis on the anatomy of the chest.[5] It decreases the chest wall and lung compliance, which restricts the amount of available space for pulmonary alveolar growth and in turn causes more labored breathing during exercise and sleep. In severe cases, these effects cause a reduction in total lung capacity (TLC), which can lead to chronic respiratory
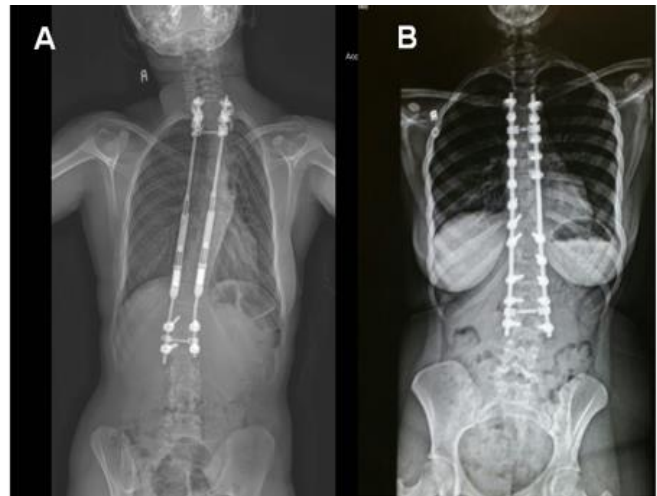


**Figure 1. Comparison of MAGEC and Spinal Fusion Surgery.** Two X-ray images highlighting the differences in corrective procedures for adolescent scoliosis. (A) shows MAGEC, an impermanent solution that utilizes an adjustable rod which extends and retracts along the spine using a magnetic controller. (B) displays spinal fusion, a permanent solution which forces the sine to remain the same length.

complications including pulmonary hypertension and respiratory failure.[6]

The main approach to correcting spine curvature and allowing proper development of the chest wall is surgical in nature, involving a procedure called "spinal fusion" which fuses the vertebrae together (Figure 1B). Metal implants are used to hold the spine in place as the vertebrae fuse into a single, solid bone.[7] This corrects existing deformity and prevents further curvature of the spine. The use of spinal fusion in young children who have not fully developed their chest wall may result in stunted growth of the thorax and consequently decreased lung function. Thus, there exists an alternative surgical treatment for children who have not developed enough lung capacity for spinal fusion. This method is called the Magnetic Expansion Control (MAGEC) Spinal Growing Rod, a system of implantable rods with an external remote control that braces the spine and allows continuous growth by magnetic lengthening of the spine every three to six months[8] (Figure 1A).

The post-spinal fusion surgery wielding of the spinal vertebrae into a single, solid bone causes stunted development by limiting the spine's ability to lengthen with growth. This fusion in turn disallows the expansion of the mediastinum, which ultimately stunts the growth of the lungs. Limited lung growth in children who receive spinal fusion surgery can lead to pulmonary paralysis or even death.[5] Thus, routine spinal fusion in children with scoliosis is not recommended at an early age. For children with scoliosis that are in an intermediate age range in which they may have developed enough lung capacity for sufficient pulmonary function after spinal fusion, it is necessary to know the exact stage of lung development. This may be estimated by measuring TLC.

Current approaches to measuring TLC include pulmonary function tests (PFT) and using computerized tomography (CT) scans to create images for calculating TLC. However, a first-hand account from a physician at the University of Virginia revealed that PFTs are not used to measure TLC in children with scoliosis because the patients are often too young to comply with protocol and correctly blow into the measuring device.[9,10] Additionally, using CT scans to calculate lung volume poses as a high risk of radiation to pediatric patients.[11,12] Thus, there is a need for a safe and accurate method of obtaining TLC measurements in children with scoliosis in order for physicians to determine the safest and most effective plan of treatment for these patients.

Our solution to this problem was to develop a user-friendly computational framework to enable lung volume calculation from X-ray images. X-ray scanning is the preferred method of obtaining patient TLC as CT scanners use 100 to 500 times more radiation than conventional X-rays. Our solution consists of two major parts: (1) obtaining and validating mediastinal volumes from patient CT scans, and (2) developing a 3D ribcage model to measure thoracic volume from patient X-rays. From here, future Capstone groups will be able to calculate lung volume by subtracting the mediastinal constant from thoracic volume and automate lung volume calculations by implementing a neural network to identify features of X-rays. This solution will provide safer, affordable, and accessible healthcare to the patients with scoliosis.

## Results

The focus of this project was centralized around obtaining standardized values and models necessary for calculating lung volumes from patient X-rays. In order to do so, the project was broken into two parts: establishing mediastinal constants and constructing standardized 3D ribcage models. The first part concentrated on developing and verifying mediastinal constants for various patient biometrics including age, sex, weight, and height. The second part of the project focuses on constructing a 3D ribcage model from CT scans as a preliminary step in creating standardized models for patients.
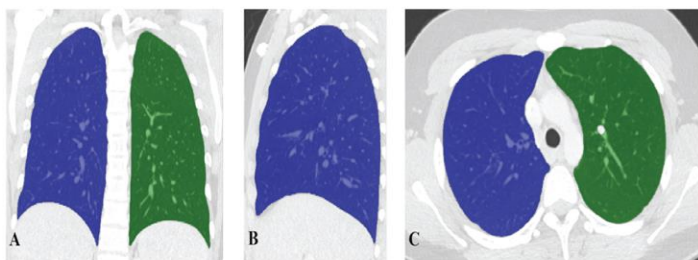


**Figure 2. Lung Identification and Segmentation** Lung segmentation using the Pulmonary Function Toolkit in MATLAB. The right and left lungs are highlighted in blue and green, respectively. Panel A is the coronal view, panel B is the sagittal view, and panel C is the axial view. Everything in the chest between the lungs is the mediastinum.

*Mediastinal Constants*

Calculating Mediastinal Volume from CT scans

The mediastinal volume calculations were computed in MATLAB using the Pulmonary Toolkit. This process starts with a stack of CT scans that is processed to obtain segmented lobes (Figure 2). The Pulmonary Toolkit finds the lung boundaries and sections the lungs into segments. Then, the area between the two lungs is calculated for each CT slice and compiled into a single volume. This volume represents the mediastinal volume. The mediastinal volume is the space in the chest that does not include lung matter such as the heart, esophagus, and trachea.

A total of 179 patient CT scans were obtained and analyzed using the method described above. Of the CT images obtained, 11 of them could not be segmented or were missing important patient measurements. These data points were excluded from the analysis. It is expected that this volume is larger and directly proportional with increasing age and weight (Figure 4). This trend remains consistent when sex is simultaneously factored in (Figure 3). In

addition, male mediastinal volumes are on average larger than female mediastinal volumes.

Validation of Mediastinal Volumes

True mediastinal volumes cannot be directly obtained from a CT scan or another imaging technique in a clinical setting. Thus, validation methods for the values are limited. The best validation tactic is to compare the mediastinal volumes of healthy and scoliotic patients and statistically determine the differences between populations; however, a similar dataset with scoliotic patients was not available. For this dataset, a series of linear regressions were applied to measure the weight of various factors on the mediastinal constant (Figure 4). Weight was found to be the best predictor of mediastinal volume for both males and females. The r squared for the female dataset was 0.2306 for weight compared to an r squared of 0.1805 for age.

The r squared for the male dataset was 0.5401 for weight compared to an r squared of 0.5045 for age. Although weight is the best predictor, when both age and weight are
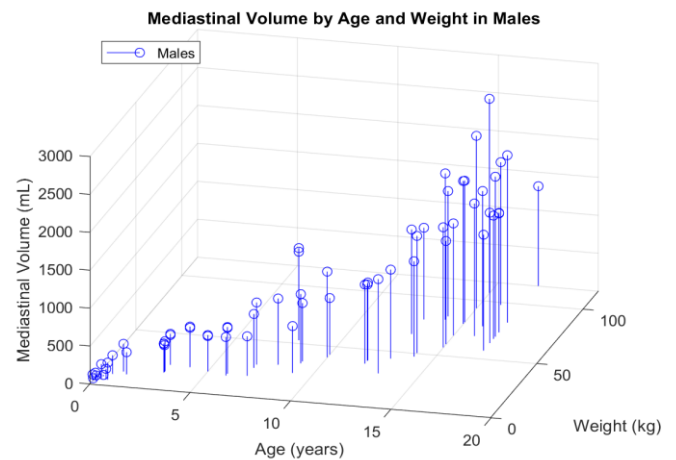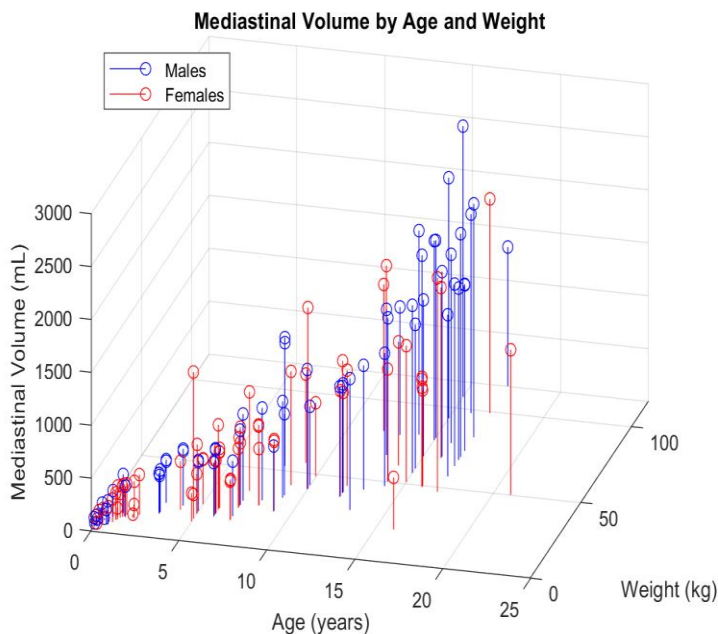


**Figure 3. Mediastinal Volumes in Context of Age, Weight, and Sex.** These graphs show the mediastinal volumes according to three factors: age, weight, and gender.

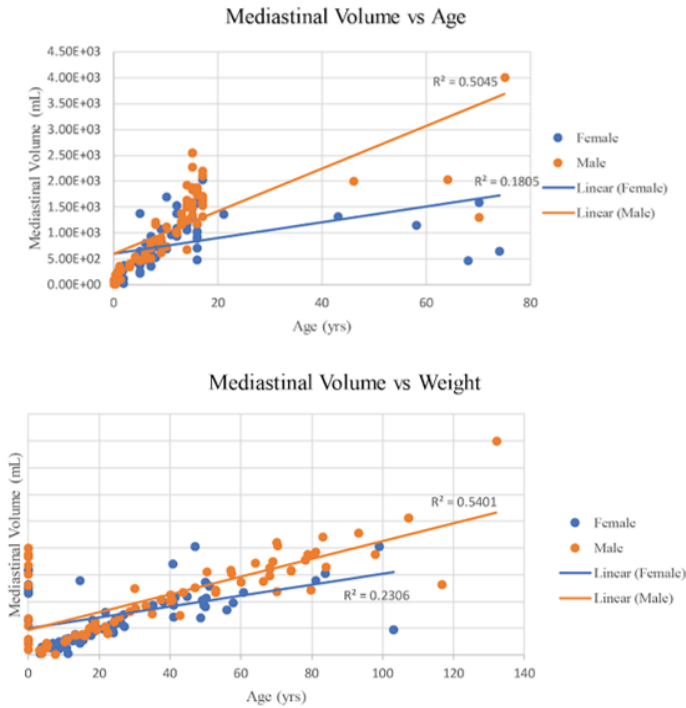taken into account, the mediastinal volume prediction was more accurate.



**Figure 4. Mediastinal Volumes vs Age and Weight.** The mediastinal volumes were plotted against age and weight to visualize the effect of each factor. A linear regression was fit to the data to measure the effect of each factor on volume.

In order to validate the results, we used cardiac volumes from literature sources as controls because the heart makes up the largest portion of the mediastinum. Although this may be the best control set of values, it is still important to note that these values are an underestimation of the true mediastinal volume. In addition, the control dataset is significantly smaller. The control dataset was composed of 19 patients, both male and female, with weights ranging from 2 to 77 kg.[13] Table 1 shows the statistical comparison of the controls with the mediastinal volume data obtained from our calculations. To add on, boxplots of specific weight groups and corresponding mediastinal volumes are shown in Figure 5, where (*) indicates statistical significance of mediastinal volumes compared to the controls. Groups were categorized based on weight and gender because they are the leading affecting factors for cardiac volume.[13] The p-values of the analysis range from close to zero to 0.439, where p-values less than 0.05 are statistically significant. A 0.05 significance level was used because it is generally accepted as an accurate way to account for difference; however, in selecting any

significance level, error may appear in two forms: as either rejecting a null hypothesis that is actually correct, or failing to reject a null hypothesis that is false. In addition, some weight ranges had a limited number of samples which could skew the results.

**Table 1. T-tests of Mediastinal and Cardiac Volumes**

| Sex | Weight Range (kg) | p-value | Sex | Weight Range (kg) | p-value |
|---|---|---|---|---|---|
| F | 3.0 - 4.0 | 0.20459 | M | 3.0 - 4.0 | 0.43958 |
| | 4.0 - 7.0 | 0.09377 | | 4.0 - 10.0 | 0.12751 |
| | 7.0 - 10.0 | 0.16110 | | 10.0 - 13.0 | 0.10181 |
| | 10.0 - 13.0 | 0.01876* | | 13.0 - 16.0 | 0.00009* |
| | 13.0 - 16.0 | 0.12542 | | 16.0 - 19.0 | 0.00017* |
| | 16.0 - 19.0 | 0.00030 | | 19.0 - 22.0 | 0.00056* |
| | 19.0 - 22.0 | 0.07076 | | 22.0 - 25.0 | 0.14191 |
| | 22.0 - 25.0 | 0.0000003* | | 25.0 - 30.0 | 0.00212* |
| | 25.0 - 30.0 | 0.00161* | | 30.0 - 40.0 | 0.00161* |
| | 30.0 - 40.0 | 0.00004* | | 40.0 - 50.0 | 0.00023* |
| | 40.0 - 50.0 | 0.00003* | | 50.0 - 60.0 | 0.00009* |
| | 50.0 - 60.0 | 0.00282* | | 60.0 - 70.0 | 0.00025* |
| | 60.0 - 70.0 | 0.15769 | | 70.0 - 80.0 | 0.00001* |

This table shows the p-values of t-tests performed comparing the mediastinal volumes to cardiac volumes from literature sources (*significance of $p < 0.05$). Results are grouped by weight and gender.
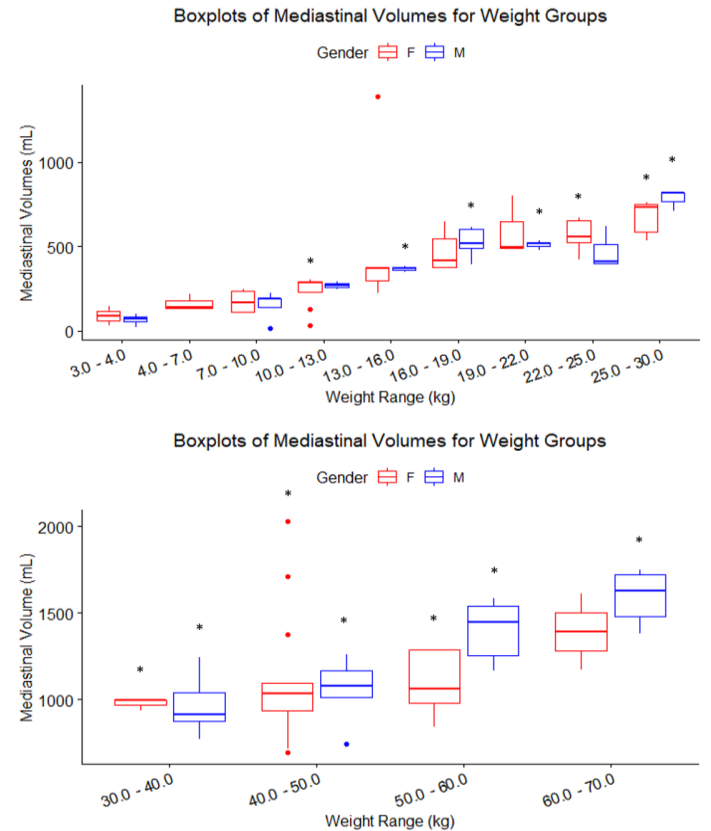


**Figure 5. Mediastinal Volumes and Weight Groups.** This shows the mediastinal volumes of specific weight groups based on literature sources of heart volumes. (*significance of $p < 0.05$).

### *3-Dimensional Ribcage Model*

<u>Construction of Ribcage Model from CT Scans</u>

In order to create a standardized ribcage model from CT scans, several methods were applied in the reconstruction. First, the Image Processing Toolbox was used to create the first model from an adult CT scan. This toolkit included two main features which were used to reconstruct the ribcage: the maximum intensity projection (MIP) feature and the volume rendering feature. In Figure 6A, the model was constructed using MIP. This model highlights the bony structures from the CT scan and smoothens the structures. Figure 6B, shows the model constructed from the volume



**(A)**



**(B)**

**Figure 6. Comparison of 3D Ribcage Models.** The 3D ribcage models were constructed using two different features from the Image Processing Toolbox in MATLAB. The first method was the maximal intensity projection (A) and the second technique was the volume rendering method (B).

rendering feature. This model also captures the bony parts from the CT scan and renders the structures in a 3-dimensional space. While both features show the spine and ribs, each method has its limitation in accurately displaying the ribcage. The MIP model strongly illuminates metal implants, as seen in the patient's spine in Figure 6A. The intensity of metal implants from surgical procedures, not necessarily related to spinal intervention, may interfere with the model capturing the bone structures of CT scans. The volume rendering method displays irregular and rough representations of the bone structure. It also captures some soft tissue such as the tissue around the spine in Figure 6B. However, the metal implants in this model are not over exposed and do not interfere with the spinal construction. Further experimentation will need to be conducted in order to determine which reconstruction method is optimal for building the standardized ribcage model from CT scans.

<u>X-ray Image Clustering</u>

Following the creation of the 3D ribcage model, chest X-rays were used to gather coordinates of the ribs in order to tailor the standardized models for patients. Figure 7A shows the original post-anterior X-ray of an adult patient with spinal surgery. Figure 7B shows the result of clustering the image pixels by four groups. The patient's metal implants are highlighted in green as seen along the spine and in the jaw. The bony structures, such as the skull and part of the ribs, are colored in light blue while the soft tissues are colored in dark blue. The background and dark areas are colored in yellow. The limitation of this technique is that it assumes each cluster group has a roughly equal number of observations, which is not the case for X-rays.[14] While the clusters can separate general areas of the X-ray image into different colored groups, the distinction between borders are blurred. Further testing will need to be conducted in order to clean up the clustering for differentiating between tissue types; however, this is a promising technique to obtain X-rays coordinates for morphing the standardized ribcage model to individual patients.

### **Discussion**

This research project has three major limitations. First, mediastinal volumes cannot be directly obtained from CT scans or other imaging techniques; therefore, "true" mediastinal values are unknown. This results in a limitation for validating the mediastinal constants calculated in this paper. However, to minimize this restraint we compared the mediastinal volume of healthy and scoliotic patients and statistically determined the differences between specific
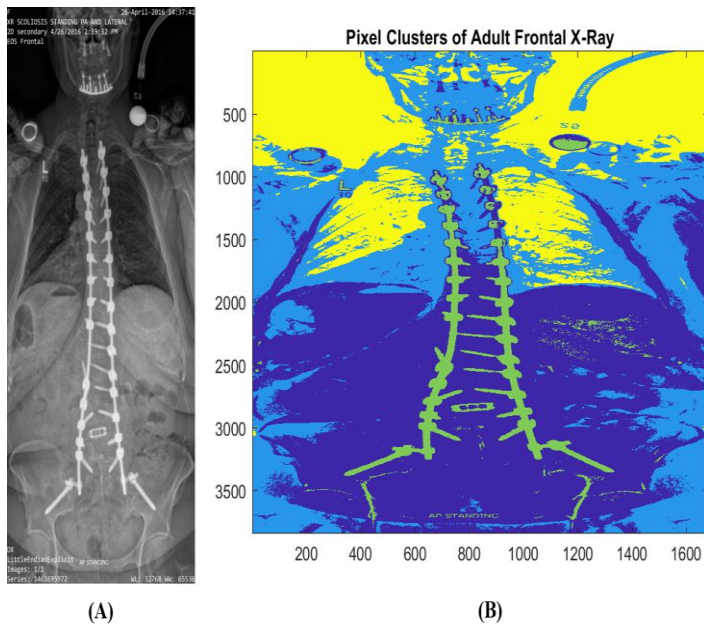
**Figure 7. Clustering of X-ray Image.** An adult post-anterior (PA) X-ray was used to cluster pixel values using the kmeans algorithm (A). The resulting clustering colormap shows pixels groups into four colors: green, light blue, dark blue, and green (B).

weight populations. The second limitation was the clustering technique used identify rib coordinates in the X-ray images. This technique assumes that each cluster group has a roughly equal number of observations, which is not the case for X-rays. Since this is a critical assumption used by the operating tool, the images will need to be cleaned up before it can be processed by the kmeans algorithm. Lastly, the number of CT scans across different age groups was also a limitation. While we had 179 scans available, about 25% of these images were from children ages 1 day old to 4 years old. The concentration of images around this age group hindered our ability to confidently establish a mediastinal constant for all age groups of patients. We believe that further projects that have access to more CT scans can markedly improve their lung volume calculation estimation by minimizing this limitation.

At the start of this project, we expected an increase in mediastinal volume with increasing factors such as age and weight. We also expected no significant difference between control values (heart volume from literature sources) and measured mediastinal volume values. Our results showed that weight was found to be the best predictor of mediastinal volume for both males and females. When both age and weight are taken into account, the mediastinal volume prediction is more accurate. There is also an increasing trend in mediastinal volume with both increasing age and weight.

We also constructed a preliminary ribcage model but there is room for improvement in several areas. Further work in this field should focus on evaluating the differences between using maximum intensity projection and volume rendering in order to develop the best representation of the ribcage from CT scans. Additionally, better clustering and capturing of bone structures from images could be achieved by increasing the quality of the X-ray DICOM images. Lastly, lining up the coordinates from the clustering to the 3D standard model can aid in acquiring lung volume by subtracting mediastinal volume from thoracic volume.

In this project, we established steps towards developing a novel method for measuring lung volume from X-ray images. Specifically, we measured mediastinal constants and created a 3D ribcage model that can be fitted on X-ray images. Further work in this field will allow physicians to calculate lung volume from X-ray images as opposed to CT scans. This is beneficial because it reduces a patient's exposure to harmful radiation and aids physicians in making better informed decisions about spinal fusion surgery for adolescent scoliosis patients.

## Materials and Methods

### Mediastinal Constants
The Pulmonary Toolkit in MATLAB was used to segment the left and right lungs. The boundaries of the lungs were estimated and used to identify the level of the diaphragm and the first lung segmentation. Then the stack of CT images was passed into a function to calculate the volume between the two segmented lungs. In each slice, gaps were filled in that may have been missed from the Pulmonary Toolkit processing. Four corners of the lungs were identified and used as boundaries of the mediastinal space. This was accomplished by incorporating Bresenham's line algorithm which calculates all intermediate points over the interval between the start and end points. This area was identified in all of the CT slices and stacked to acquire the total mediastinal volume.

### Dataset
The dataset obtained for this project was deidentified in compliance with the IRB filing and was provided by Dr. Keith Bachmann. Originally, the dataset consisted of 179 deidentified patient CT and X-ray scans of varying age, sex,

| Male | | | | |
|---|---|---|---|---|
| Age | Weight (Kg) | Age (cont.) | Weight (cont.) |
| 17 | 57.23 | 3 | 22.2 |
| 16 | 0 | 9 | 24.13 |
| 16 | 97.69 | 5 | 19.23 |
| 15 | 59.96 | 13 | 30 |
| 15 | 57 | 16 | 0 |
| 15 | 80.2 | 10 | 42.64 |
| 16 | 69 | 3M | 5.28 |
| 8 | 52.7 | 14 | 47 |
| 5 | 19.23 | 7 | 28.67 |
| 4 | 21.68 | 5M | 5.56 |
| 3 | 15.1 | 4M | 5.33 |
| 3 | 15.69 | 6 | 18.78 |
| 3 | 22.2 | 15 | 107.15 |
| 3 | 16.32 | 17 | 70 |
| 17 | 68 | 14 | 84 |
| 17 | 0 | 75 | 132 |
| 17 | 74 | 64 | 70.3 |
| 17 | 116.69 | 46 | 0 |
| 16 | 78 | 70 | 0 |
| 15 | 78.69 | 6 | 18.77 |
| 15 | 0 | 6 | 17.05 |
| 14 | 0 | 16 | 70 |
| 6M | 8.62 | 12 | 40.5 |
| 6W | 3.62 | 15 | 0 |
| 4M | 5.89 | 17 | 74 |
| 2M | 4.98 | 14 | 0 |
| 7W | 4.98 | 8M | 10.2 |
| 5W | 4.08 | 4 | 0? |
| 4M | 7.48 | 3 | 16.3 |
| 16M | 10.88 | 8 | 52.7 |
| 13M | 13.03 | 9 | 33 |
| 12M | 0 | 13 | 43.54 |
| 7M | 4.98 | 4 | 21.68 |
| 8M | 4.98 | 13 | 79.59 |
| 12M | 0 | 15 | 93 |
| 1D | 3.06 | 3 | 15.1 |
| 2M | 4.08 | 15 | 68 |
| 9M | 0 | 9 | 34.83 |
| 12D | 3.62 | 10 | 40 |
| 8M | 0 | 7 | 25.7 |
| 15M | 0 | 13 | 66.25 |
| 1D | 3.62 | 14 | 0 |
| 13M | 10.88 | 8 | 30.21 |
| 8W | 3.46 | 12 | 40 |
| 14 | 0 | 2 | 14.47 |
| 13M | 12.7 | 7 | 18.39 |
| 13M | 12.7 | 14 | 50.26 |
| 7 | 28.67 | 16 | 78 |
| 5M | 5.56 | 12 | 37.4 |
| 4M | 5.33 | 17 | 83 |
| 6 | 18.78 | 14 | 84 |
| 15 | 107.15 | 17 | 64.05 |
| 17 | 70 | 14 | 81 |

| Female | | | | |
|---|---|---|---|---|
| Age | Weight (Kg) | Age (cont.) | Weight (cont.) |
| 17 | 47 | 9 | 41.4 |
| 9 | 24.6 | 12 | 83.59 |
| 8 | 26.7 | 6 | 22.89 |
| 6 | 18.14 | 8 | 26.98 |
| 5 | 14.39 | 16 | 49.9 |
| 5 | 23.89 | 16 | 48.99 |
| 16 | 21 | 7 | 26.02 |
| 15M | 11.15 | 6 | 22.5 |
| 3M | 3.7 | 15 | 0 |
| 16 | 0 | 12 | 44.7 |
| 15 | 0 | 12 | 40.79 |
| 14 | 60.7 | 16 | 0 |
| 16 | 0 | 10 | 48.4 |
| 6M | 5.58 | 16 | 49.25 |
| 16M | 12.24 | 6 | 19.39 |
| 11M | 8.62 | 5 | 17.69 |
| 14M | 10.88 | 8 | 26.7 |
| 13M | 9.98 | 11 | 57.69 |
| 8W | 3.17 | 8 | 27 |
| 14M | 10.88 | 10 | 40.64 |
| 7M | 6.92 | 16 | 49.4 |
| 10M | 6.8 | 5 | 14.39 |
| 11M | 10.43 | 12 | 80.9 |
| 4M | 5.89 | 16 | 68.04 |
| 5M | 0 | 13 | 0? |
| 5M | 3.17 | 5 | 23.89 |
| 12M | 8.62 | 8 | 25.13 |
| 7M | 0 | 15 | 51 |
| 8W | 3.29 | 5 | 12.52 |
| 6M | 6.35 | 16 | 0 |
| 3W | 3.79 | 6 | 21.59 |
| 14M | 7.26 | 6 | 22.89 |
| 7 | 16.25 | 7 | 24 |
| 2 | 13.15 | 9 | 55.96 |
| 9 | 24.6 | 19M | 15.39 |
| 17 | 99 | 12 | 38.01 |

**Figure 8. CT Dataset.** Dataset of CT scans provided by Dr. Keith Bachmann. This included a total of 179 patients ranging from ages 1 day old to 74 years old and weights from 3 kg to 132 kg.

and weight. Of these 179 samples, 168 CT scans were successfully segmented and used for calculating mediastinal volumes (Figure 8). In the dataset, the patient ages ranged from 1 day old to 74 years old. Patient weights ranged from 3 kg to 132 kg and patient sex consisted of 89 females and 90 males.

### 3-Dimensional Ribcage Model

Construction of Ribcage Model from CT Scans

The preliminary ribcage model was built using the Image Processing Toolbox in MATLAB (Supplemental Figure 1). The toolkit displays the XY, XZ, and YZ viewpoints of the CT scans on the left panel and shows the intensity adjustment tool on the right panel. Two features were used to reconstruct the standardized ribcage model from CT scans. The first technique was the maximum intensity projection (MIP). This method projects the voxel with the highest attenuation value that falls on the parallel rays from the viewpoint to the plane of projection.[15] The second technique from the toolkit was the volume rendering function. This method uses an alphamap to display the structures from the CT scan. Each pixel rgb values are added up and sums closer to 255 are opaquer while those closer to 0 are more transparent.

X-ray Image Clustering

The X-ray image clustering was performed in MATLAB using the kmeans algorithm. The kmeans method is an iterative algorithm which partitions the dataset into k pre-defined distinct subgroups (clusters). This technique assigns data points to clusters using the minimum sum of squared distance between the data points and cluster centroid, which is the mean of all the data points that belong to that subgroup. Each data point belongs to only one group and each group is assumed to have an equal number of observations.[16] First, the X-ray image was loaded in MATLAB and the pixel values were stored in a matrix. Then the matrix was transformed into 1D array and the values were converted from the uint8 format into doubles. The array values were clustered into four groups using the kmeans algorithm and stored as new cluster values. Then, the subgroups were transformed into a matrix of the same image size and displayed as colormap.

## End Matter

## References

1. Horne, J. P., Flannery, R. & Usman, S. Adolescent Idiopathic Scoliosis: Diagnosis and Management. *AFP* **89**, 193–198 (2014).
2. Konieczny, M. R., Senyurt, H. & Krauspe, R. Epidemiology of adolescent idiopathic scoliosis. *J Child Orthop* **7**, 3–9 (2013).
3. Children's Wisconsin. Idiopathic Scoliosis in Children and Adolescent. https://chw.org/medical-professionals/tools-and-resources/medical-care-guidelines/spinal-asymmetry.
4. NIH. Adolescent idiopathic scoliosis. *Genetics Home Reference* https://ghr.nlm.nih.gov/condition/adolescent-idiopathic-scoliosis.
5. Karol, L. A. Early definitive spinal fusion in young children: what we have learned. *Clin. Orthop. Relat. Res.* **469**, 1323–1329 (2011).
6. Tsiligiannis, T. & Grivas, T. Pulmonary function in children with idiopathic scoliosis. *Scoliosis* **7**, 7 (2012).
7. Haas, M., Hamm, B. & Niehues, S. M. Automated lung volumetry from routine thoracic CT scans: how reliable is the result? *Acad Radiol* **21**, 633–638 (2014).
8. Philadelphia, T. C. H. of. MAGEC Growing Rods. https://www.chop.edu/treatments/magec-growing-rods (2016).
9. Enright, P. L. *et al.* Quality of spirometry test performance in children and adolescents : experience in a large field study. *Chest* **118**, 665–671 (2000).
10. Seoud, L., Cheriet, F., Labelle, H. & Dansereau, J. A novel method for the 3-D reconstruction of scoliotic ribs from frontal and lateral radiographs. *IEEE Trans Biomed Eng* **58**, 1135–1146 (2011).
11. NPR. How CT Scans Have Raised Kids' Risk For Future Cancer. *NPR.org* https://www.npr.org/sections/health-shots/2013/06/10/190449001/how-ct-scans-have-raised-kids-risk-for-future-cancer.
12. Fujita, N. *et al.* Impact of fusion for adolescent idiopathic scoliosis on lung volume measured with computed tomography. *Eur Spine J* **28**, 2034–2041 (2019).
13. Nghiem Quang X., Schreiber Melvyn H. & Harris Leonard C. Cardiac Volume in Normal Children and Adolescents. *Circulation* **35**, 509–522 (1967).
14. Keppel, J. Anomaly Detection: (Dis-)advantages of k-means clustering. *inovex Blog* https://www.inovex.de/blog/disadvantages-of-k-means-clustering/ (2017).
15. Fishman, E. K. *et al.* Volume Rendering versus Maximum Intensity Projection in CT Angiography: What Works Best, When, and Why. *RadioGraphics* **26**, 905–922 (2006).
16. Dabbura, I. K-means Clustering: Algorithm, Applications, Evaluation Methods, and Drawbacks. *Medium* https://towardsdatascience.com/k-means-clustering-algorithm-applications-evaluation-methods-and-drawbacks-aa03e644b48a (2019).

## Supplemental Material
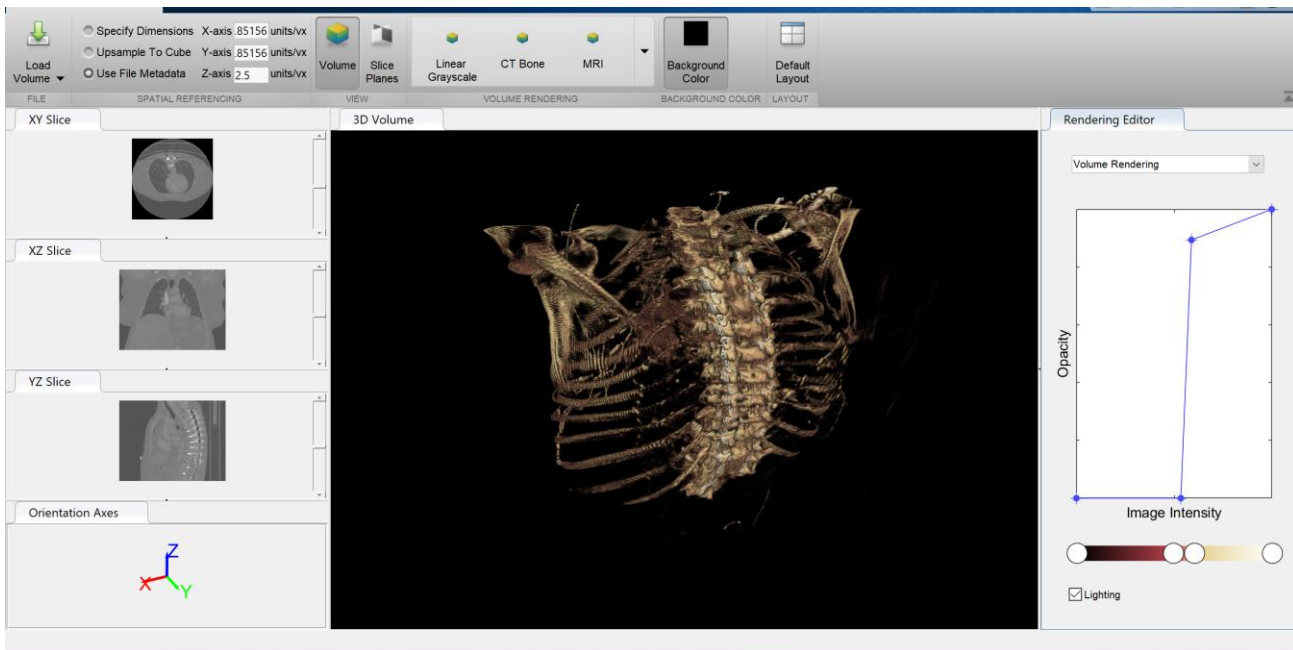


**Supplemental Figure 1. Construction of Ribcage Model from CT Scans.** The 3D ribcage was built using the Image Processing Toolbox in MATLAB. The layout of the program shows the XY, XZ, and YZ viewpoints of the patient CT scans on the left panel and the image intensity adjustment tool on the right panel.